Metal-semiconductor transition and structural change in $(BEDT\text{-}TTF)_3(ClO_4)_2$

Toshiaki Enoki, Kyozo Tsujikawa, Kazuya Suzuki, Akira Uchida, and Yuji Ohashi
Department of Chemistry, Tokyo Institute of Technology, Ookayama, Meguro-ku, Tokyo 152, Japan

Hideo Yamakado and Kuya Yakushi
Institute for Molecular Science, Okazaki 444, Japan

Gunzi Saito
Department of Chemistry, Kyoto University, Sakyo-ku, Kyoto 606, Japan
(Received 6 May 1994; revised manuscript received 19 August 1994)

A metal-semiconductor transition at $T_c = 170.4$ K in a two-dimensional organic metal, $(BEDT\text{-}TTF)_3(ClO_4)_2$, was investigated by means of ESR, resistivities, specific heats, and x-ray diffractions. The specific heats show a λ-type anomaly at T_c with a second-order nature and a large entropy change range of 3 J/K mol. In addition to the H/D isotope effects on T_c, x-ray diffraction suggests the development of an intermolecular interaction network between the ethylene groups of BEDT-TTF molecules and ClO_4^- anions below T_c. These experimental findings demonstrate that the three-dimensional structural rearrangement, which is closely correlated to the development of the intermolecular interaction network, plays an important role in the metal-semiconductor transition.

INTRODUCTION

Bis(ethylenedithio) tetrathiafulvalene (BEDT-TTF) is a TTF-type donor with ethylenedithio-substitutional groups attached to the short sides of the TTF skeleton. BEDT-TTF charge-transfer complexes give a large number of two-dimensional conductors, which have a variety of electronic states among semiconductors, metals, and superconductors.[1] The low dimensionality in the electronic structures gives rise to an instability towards semiconducting states in a large number of metallic BEDT-TTF compounds. Most of these metallic BEDT-TTF complexes which undergo metal-semiconductor transitions have transition temperatures in the temperature range around 100–200 K. Since, in a BEDT-TTF molecule, the six-membered rings of the substitutional group attached to the TTF skeleton have nonplanar structures, the substitutional ethylene groups have a degree of freedom for a bending motion. From experimental results, ethylene groups are evidenced to be thermally vibrating at room temperature for many of the BEDT-TTF complexes.[2] Moreover, the presence of intermolecular interactions between the hydrogen atoms of ethylene groups and anions is expected to give rise to correlated molecular motions between ethylene groups and anion molecules. The correlated molecular motions are quenched around the similar temperature range to the range of the metal-semiconductor transitions, so that it is deduced that there is some correlation between the molecular motions and the metal-semiconductor transitions.

$(BEDT\text{-}TTF)_3(ClO_4)_2$ is known to be one of the BEDT-TTF complexes having a two-dimensional metallic state. In the complex, BEDT-TTF donor molecules form two-dimensional conducting sheets in the *bc* plane, which are separated by the presence of ClO_4^- anions. The intermolecular interactions between the ClO_4^- anions and the ethylene groups of the BEDT-TTF donor molecule stabilize the two-dimensional stacking structure. $(BEDT\text{-}TTF)_3(ClO_4)_2$ undergoes a metal-semiconductor transition at $T_c = 170$ K, although the origin of the transition still remains unsolved.[3–8] In a metal-semiconductor transition, not only the change in the electronic system but also that in the lattice system participates in the transition behaviors, where both systems are coupled to each other through the electron-phonon interactions. Therefore, it is interesting to investigate the role of the molecular motions related to the ethylene groups and the ClO_4^- anions in the metal-semiconductor transition. In this study, in order to clarify the correlation between the molecular motions and the metal-semiconductor transition, we present the detailed investigation of the change in the electronic structures and the molecular structures through the transition by means of specific heats, electrical resistivities, ESR, and x-ray diffraction.

EXPERIMENT

Single crystals of $(BEDT\text{-}TTF)_3(ClO_4)_2$ were prepared by a standard electrochemical technique. A 3×10^{-4} mol quantity of BEDT-TTF was reacted with $(1.8\text{–}3.7)\times10^{-3}$ mol of $(C_4H_9)_4NClO_4$ in 15 ml of $C_2H_3Cl_3$ under a constant current (5 or 10 μA) for one week. Two kinds of lustrous black crystals were simultaneously produced in an electrochemical cell, which corresponded to two polymorphs, $(BEDT\text{-}TTF)_2ClO_4(C_2H_3Cl_3)_{0.5}$ and $(BEDT\text{-}TTF)_3(ClO_4)_2$. The assignment of the structures was carried out by means of x-ray diffraction. At 10 μA, thin plates of $(BEDT\text{-}TTF)_3(ClO_4)_2$ were mainly obtained. Typical dimensions of the crystals were $2\times5\times0.05$ mm^3.

The ESR spectra were measured between liquid helium and room temperatures with a conventional Varian Associates *X*-band E112 spectrometer having a TE_{102} microwave cavity. The microwave frequencies were detected by a frequency counter and the applied field was calibrated using a DPPH standard sample. The temperature control was achieved using Oxford Instruments ESR9 continuous-flow helium cryostat. The sample was mounted on a Teflon holder in a 4-mm-diam quartz ESR tube with 20-Torr He exchange gas. The microwave power supplied into a cavity was below 1 mW to avoid a saturation effect of the ESR spectra. Conductivities were measured by means of both dc four-prove and microwave techniques between liquid helium and room temperatures. In the dc method, the temperature is monitored by calibrated Pt (room temperature to 35 K) and Ge (35 K to liquid-helium temperature) thermometers. Microwave conductivities were measured with a TE_{011} cavity with a frequency of 9.4 GHz, where the temperature was monitored using Pt and Ge thermometers. Specific heats were measured from 30 K to room temperature using an ac technique with a frequency of 3 Hz, where ac temperature variations were detected by means of 0.025-mm-diam chromel-alumel thermocouples, the absolute values of which were regulated to be typically $\Delta T = 0.007$ K. The thermocouples were cemented to a platelet sample with GE7031 vanish. The temperature of the heat bath was monitored by a calibrated Pt thermometer. Absolute values of specific heats were obtained using a gold thin plate as a standard. X-ray diffractions were investigated in the temperature range 120 K to room temperature with an automated Rigaku AFC5 four-circle diffractometer equipped with a liquid-nitrogen cryostat.

EXPERIMENTAL RESULTS

Temperature dependence of dc and microwave conductivities are presented in Fig. 1 for electrical conduction in the conducting *bc* plane. The vector for the microwave electric field is in the plane for the microwave conductivity measurements. The behaviors of both conductivities indicate an onset of a metal-semiconductor transition at 170 K. In the dc conductivity trace, we observe a small hump just at the transition temperature accompanied by a steep drop on the low-temperature side. For the phase

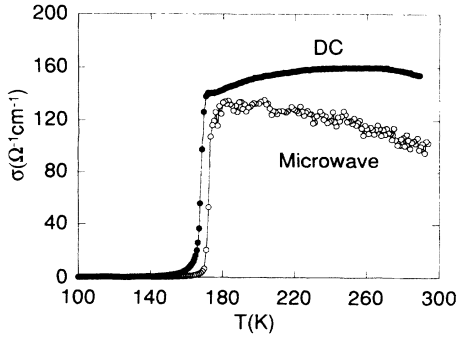

FIG. 1. Temperature dependence of in-plane conductivities σ measured by dc and microwave (9.4 GHz) techniques. The electric field of the microwave is applied in the *bc* plane.

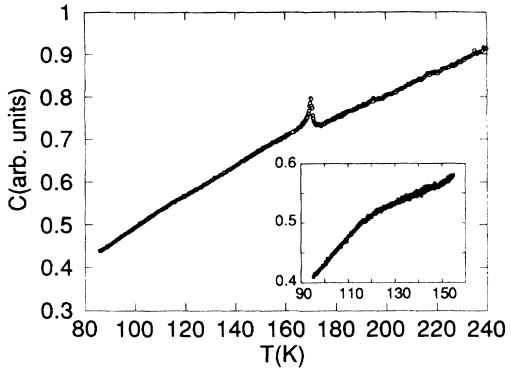

FIG. 2. Temperature dependence of specific heats *C*. The inset shows a detailed behavior of the anomaly around 120 K.

transition, we estimate the activation energy to be $E_a = 1000$ K in the temperature range below 130 K, which is well below the transition.

In Fig. 2, we show the results of specific heats *C* as a function of temperature in a heating run with a heating rate of 0.5 K/min. There are two anomalies in the specific heat vs temperature curve. A metal-semiconductor transition was observed at $T_c = 170.4 \pm 0.3$ K (average for two samples) as a λ-type anomaly, whose magnitude ranges about 10% of the total specific heat at T_c. In addition to the metal-semiconductor transition, a small hump with a broad shape was observed around 120 K. No appreciable difference is observed in the behavior of specific heats between heating and cooling runs. The annealing of a sample for 5 h just below T_c (~ 140 K) in a cooling run does not modify the shape of the specific-heat peak for a subsequent heating run. In addition, no hysteresis was observed for all the runs in the specific-heat measurements. Therefore, the metal-semiconductor transition is considered to be classified into a second-order phase transition. The anomaly at the metal-semiconductor transition has an isotope effect between the complexes with h_8-BEDT-TTF and d_8-BEDT-TTF donors, as shown in Fig. 3. Here, h_8-BEDT-TTF denotes a BEDT-TTF molecule with ethylene groups consisting of light hydrogen atoms, while, in a d_8-BEDT-TTF molecule, all the hydrogen sites in the ethylene groups are substituted with deuterium atoms. The complex with d_8-BEDT-TTF donors has T_c at 171.7 ± 0.5 K (average among three samples), which is 1.3 K higher than that of the h_8-BEDT-TTF one. The difference in the transition temperature associated with the H/D isotope effect is reproducible for the measurements with several samples. The trend of the H/D isotopes effect is opposite from that for ordinary superconductors,[9] but is similar to that for transitions of ferroelectric materials such as KH_2PO_4/KD_2PO_4.[10–12] Figure 3 also shows the resistivity ρ results for the complexes with d_8- and h_8-BEDT-TTF's. The $d \ln\rho/dT$ vs T plot shows that the difference in the transition temperatures is 1 K between the two kinds of complexes, which is in good quantitative agreement with the H/D isotope effects obtained in the specific-heat measurements.

$(BEDT\text{-}TTF)_3(ClO_4)_2$ has a triclinic crystal structure ($P\bar{1}$) with the following lattice parameters: $a = 16.463$

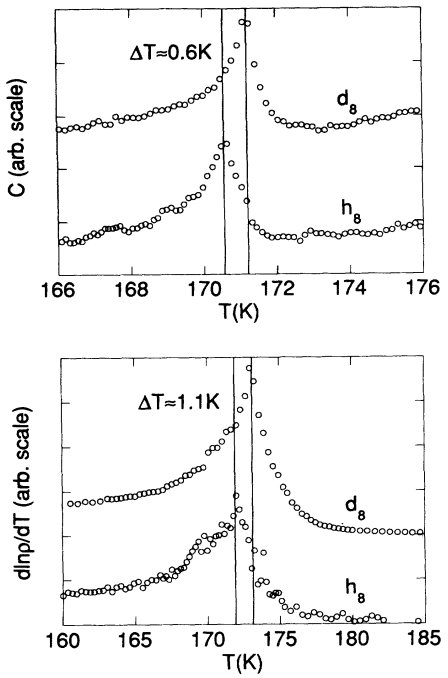

FIG. 3. H/D isotopes effects of the specific heats C and resistivities ρ in the vicinity of the metal-semiconductor transition temperature. The vertical solid lines indicate the positions of the transition temperatures. ΔT is the difference in the transition temperatures between the h_8-BEDT-TTF and d_8-BEDT-TTF compounds. The plots for the d_8-BEDT-TTF compounds are shifted upward for clarity.

Å, $b=9.498$ Å, $c=7.613$ Å, $\alpha=95.91°$, $\beta=87.17°$, $\gamma=90.84°$, $z=1$, $V=1182$ Å,^{3} as shown in Fig. 4.[3] A unit cell involves three BEDT-TTF molecules, one of which (A) is located on an inversion center. The other two molecules (B), which are located at general points in a unit cell, are equivalent with each other through the inversion symmetry. The molecular planes of these BEDT-TTF molecules are oriented approximately perpendicular to the bc plane. The temperature dependence of the lattice constants are investigated. On the lowering of the temperature, the lattice parameters a, b, and c decrease monotonically with no discontinuous change at T_c. This fact proves the second-order nature of the metal-semiconductor transition. The angle α between the b and c axes shows a steep decrease at T_c, indicating a change in the arrangement of the BEDT-TTF molecular plane. Figure 5 gives the temperature dependence of thermal contraction of the lattice constants for three crystallographic axes a, b, and c. The results show an anisotropic thermal contraction behavior among these three axes. The thermal contraction of the b axis in the conducting bc plane is small, which is comparable to that of the a axis ranging $\sim 0.2\%$ from room temperature to 230 K. The c axis, which is another crystallographic axis in the conducting plane, has a larger thermal contraction by about five times than the other two axes. This means that the unharmonicity of the molecular motions is most pronounced in the c-axis direction among all the directions.

Next, we show the results of the ESR measurements. The shape of the ESR signal has temperature and angular dependence in the whole temperature range. Above the metal-semiconductor transition temperature, ESR spectra have asymmetric Dysonian line shapes when an oscillating electric field of a microwave is applied parallel to the bc plane, which forms a two-dimensional conducting plane. In other cases, symmetric Lorentzian line shapes are observed even in the metallic state above T_c except the critical region in the vicinity of T_c. Figure 6 shows temperature dependence of the asymmetry parameters A/B for the applied magnetic field parallel to three axes a^*, b, and c^*. In these measurements, the oscillating electric field of the microwave is oriented parallel to the applied static magnetic field. The asymmetry parameter A/B, which is a parameter representing the line shape of the ESR signal, is shown to depend on the directions of the oscillating electric field, while the static magnetic field gives minor effects on the line shapes. In Fig. 6(a) where the oscillating electric field is applied perpendicular to the conducting bc plane, the shape of the ESR signal is Lorentzian and A/B becomes unity in the whole temperature range except the critical region in the vicinity of T_c in which A/B increases anomalously, suggesting a deviation of the line shape towards Dysonian. In Fig. 7

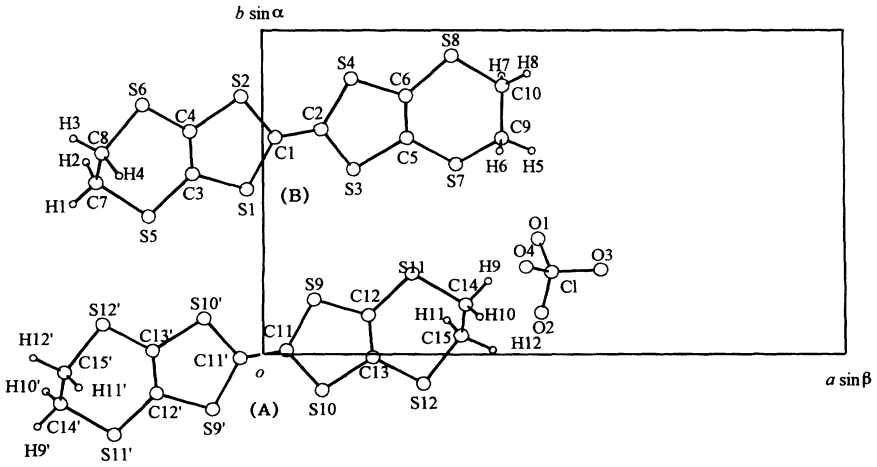

FIG. 4. The molecular arrangement of the BEDT-TTF molecules and the ClO_4^- anions in the a^*b plane after Ref. 3. BEDT-TTF molecule A is on an inversion center.

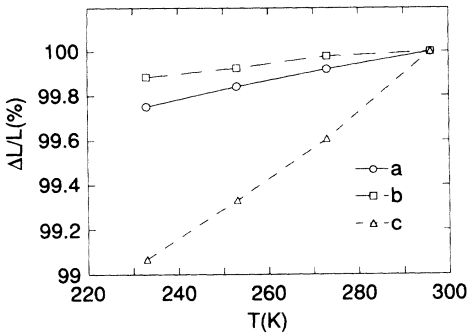

FIG. 5. Thermal contraction $\Delta L/L$ of the lattice constants for the three crystallographic axes ($L=a,b,c$). The data are normalized at 296 K.

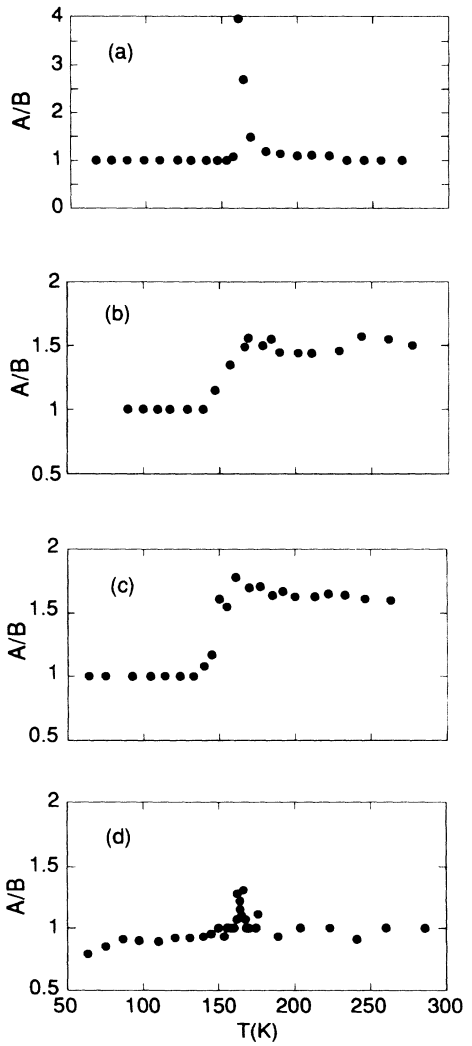

FIG. 6. Temperature dependence of asymmetry parameters A/B of the ESR line shape where the oscillating electric field of the microwave is applied parallel to the a^*, b, or c^* axis for (a), (b), or (c)/(d), respectively. For the electric field parallel to the c^* axis, we employ thick (c) and thin (d) samples.

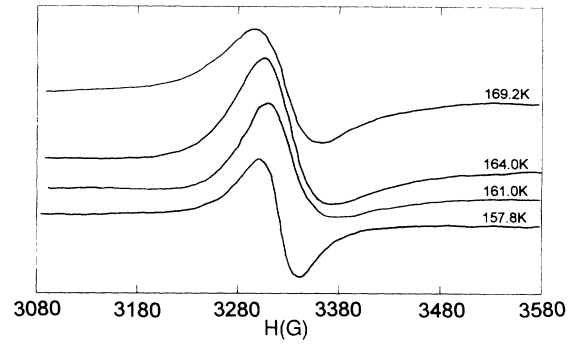

FIG. 7. The line shapes of the ESR signals in the vicinity of T_c for the oscillating electric field applied parallel to the a^* axis.

is shown the drastic change in the line shape from Lorentzian to Dysonian in the critical region around T_c. The anomalous change in the line shape in the critical region is discussed in the next section. Figures 6(b) and 6(c) give temperature dependence of A/B for the oscillating electric field parallel to the b and c axes, respectively, in the conducting bc plane. The asymmetry parameter A/B has a constant value ranging around 1.5 above T_c, which means the Dysonian shape of the ESR signal. Below T_c, A/B becomes unity, suggesting the Lorentzian line shape of the signal. In the metallic region above T_c, the observed asymmetric line shapes are considered to be associated with high in-plane conductivity having a magnitude of 30–40 $\Omega^{-1}\,\mathrm{cm}^{-1}$. The skin depth of the microwave is given in the following equation:

$$\delta = c(2\pi\omega\sigma)^{-1/2}\,, \tag{1}$$

where δ is the skin depth when the microwave penetrates the bc plane. ω and σ are the microwave frequency and the in-plane conductivity, respectively. The skin depth δ is estimated to be ~ 0.1 mm, using $\omega = 9$ GHz (X-band frequency) and the in-plane conductivity value. Since the thickness of the sample we employed in these measurements [Figs. 6(a)–6(c)] is ~ 0.1 mm, the asymmetric Dysonian line shape is explained in terms of the skin depth effect. In the experiment with a thinner sample having a thickness of 0.05 mm, the line shape becomes symmetric in the whole temperature range except in the critical region as shown in Fig. 6(d). This is also consistent with the presence of the skin depth effect in the metallic region.

We show information on the g values. In general, an asymmetric line shape is realized by mixing the dispersion contribution X' into the absorption contribution X'' in the ESR signal. In order to get an intrinsic behavior of the g values, we need to extract the absorption contribution X'' by means of the deconvolution of the spectra with the two contributions, as expressed by the following equation:

$$F(H-H_r) = xX''(H-H_r) + (1-x)X'(H-H_r)\,, \tag{2}$$

$$X'(H) = \frac{1-H^2}{(1+H^2)^2}\,, \tag{3}$$

$$X''(H) = \frac{2H}{(1+H^2)^2}\,, \tag{4}$$

where H_r, $F(H)$, and x are the central field of the resonance, the observed line shape, and the fraction of the absorption contribution, respectively. Figure 8 presents the temperature dependence of the g values for the magnetic field applied parallel to the a^* and c^* axes, which are obtained after the line-shape correction. The g values are independent of temperature well above and below T_c, while the g values show steep changes in the vicinity of T_c. It is difficult to analyze g tensors in detail in the metallic phase above 170 K, since the ESR signal has an asymmetric Dysonian shape due to a good electrical conduction, even though the line-shape correction is made. Therefore, we give the g tensors and their principal axes only at 90 K in Table I, which are obtained by the angular dependence of the ESR signals. The g tensors, which are in a similar range to the g values for typical BEDT-TTF complexes,[13] suggest the BEDT-TTF molecular long axis oriented almost parallel to the a^* direction, consistent with the crystallographic data.[3]

DISCUSSION

Here, we discuss the correlation between the metal-semiconductor transition and the change in the structure induced by the transition. The result of the specific heat suggests the second-order nature of the phase transition, as mentioned in the previous section. In order to clarify the nature of the transition more clearly, we estimate the entropy change ΔS associated with the metal-semiconductor transition. In order to extract the anomalous contribution caused by the transition, we take a linear base lines whose ends are both smoothly connected to the specific heat values at 140 and 230 K. The anomalous contribution is obtained by subtracting the base line (normal contribution) from the total specific heat. The entropy change associated with the anomalous specific heat contribution is shown in Fig. 9. The continuous change in the entropy is consistent with the second-order nature of the transition. As seen in Fig. 9, the total entropy change concerning the contribution is estimated to be 3 J/K mol, 60–70 % of which is consumed below T_c. The observed large entropy consumption below T_c, suggesting a weak short-range-order effect above T_c, is indicative of the three-dimensional character of the transition.[14] The estimated total entropy change associated with the metal-semiconductor transition is about 1 order of magnitude larger than that in ordinary organic metals such as TTF·TCNQ (0.4 J/K mol) (Refs. 15 and 16) where the change in the electronic system plays a major role in the metal-semiconductor transition. The spin paramagnetic susceptibility $\chi_s = 3.7 \times 10^{-4}$ emu/mol in the metallic phase[6] suggests that the electronic entropy above the transition temperature is expected to have a similar value to the observed entropy change, according to the following relation between the electronic entropy S_e and the density of states $D(E_F)$ at the Fermi energy E_F:

$$S_e = \frac{\pi^2}{3} k_B^2 D(E_F) T \ . \tag{5}$$

However, the experimental results mentioned above and the structural analyses[17,18] require a strong contribution of a structural change to the metal-semiconductor transition, as well as the change in the electronic structure. In this respect, the H/D isotope effects on the transition temperature mentioned in the previous section give important information. Namely, the difference in T_c between h_8-BEDT-TTF and d_8-BEDT-TTF complexes suggests that the molecular arrangement of the ethylene groups is closely correlated to the metal-semiconductor transition. In other words, the hydrogen sites of the ethylene groups in BEDT-TTF molecules are considered to be affected by the structural change induced by the metal-semiconductor transition.

In order to know the possible structure change caused by the metal-semiconductor transition, we compare the structures between the metallic and semiconducting phases. Kobayashi *et al.* suggested the presence of thermal motions of the ClO_4^- anions and the ethylene

TABLE I. The g-tensor components and their principal axes at $T = 90$ K. The polar angle θ is measured from the a^* axis, while the azimuthal angle ϕ from the b axis in the bc^* plane.

	g value	θ	ϕ
g_{xx}	2.0123	15.0	−28.2
g_{yy}	2.0005	76.8	119.4
g_{zz}	2.0070	82.3	−148.8

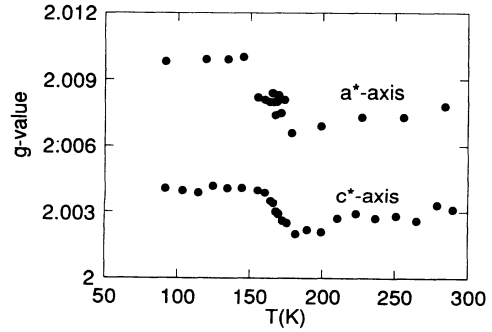

FIG. 8. Temperature dependence of the g values parallel to the a^* and c^* axes obtained after the line-shape correction.

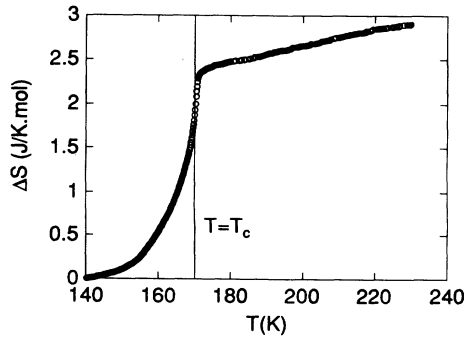

FIG. 9. Temperature dependence of the entropy change ΔS associated with the metal-semiconductor transition. The vertical solid line indicates the position of T_c.

TABLE II. The isotropic thermal parameters (Å^2) of the constituent atoms in the ClO_4^- anion after Refs. 17 and 18. See Fig. 4 for the positions of the oxygen atoms.

	Room temperature	120 K
Cl	3.94	1.32
O_1	15.23	3.20
O_2	7.80	3.17
O_3	5.46	1.78
O_4	10.10	2.18

groups of the BEDT-TTF molecules at room temperature, from the x-ray crystal structure analysis,[17] while the experiments by Mori[18] proves the incomplete quenching of the thermal motions at 120 K, which is well below T_c. We show the crystal structure of $(BEDT\text{-}TTF)_3(ClO_4)_2$ in Fig. 4 for the assistance of understanding the crystal structure modification associated with the metal-semiconductor transition. The thermal parameters and the interatomic distances of the ClO_4^- anion are summarized in Tables II and III after Refs. 17 and 18. The thermal parameters of the constituent oxygen atoms become drastically small as the temperature goes down from room temperature to 120 K through the metal-semiconductor transition. Remarkable changes occur for the thermal parameters of the three oxygen atoms O_1, O_2, and O_4. Taking into account the fact that the thermal parameter of the oxygen atom O_3, where the bond Cl-O_3 is almost parallel to the a^* axis or approximately parallel to the molecular long axis of the BEDT-TTF molecule, has the smallest value of the thermal parameters among the oxygen atoms, the thermal vibration, which is described in terms of a hindered rotation with the rotational axis parallel to the a^* axis, is quenched by the onset of the phase transition, although the thermal motions still exist even in the temperature range below T_c. The thermal motions of the ethylene groups are also affected by the onset of the transition.[17,18] According to Refs. 17 and 18, the thermal parameters of the carbon atoms at the ethylene groups, whose values range around 3 Å^2 at room temperature, are reduced to be about one-third of the room-temperature values at 120 K. This finding suggests that the bending motion of the ethylene group is quenched by the onset of the transition. Next, we show changes of the interatomic distances in the ClO_4^- anion, which are summarized in Table III after Refs. 17 and 18. The quenching of the molecular motions below T_c induces the elongation of the interatomic distances between Cl and O atoms in the ClO_4^- anion. The elongation of the interatomic distances is considered to be realized by the enhancement of the intermolecular interactions between the ClO_4^- anions and the BEDT-TTF molecules. Consequently, the network of the intermolecular interactions becomes strengthened at the expense of the intramolecular interactions in the ClO_4^- anions. The evidence of the development of the intermolecular interaction network associated with the quenching of the molecular motions of the ClO_4^- anions appears in the shortening of the interatomic distances between the hydrogen atoms of the ethylene groups in the BEDT-TTF molecules and the oxygen atoms of the ClO_4^- anions, as summarized in Table IV (Refs. 17 and 18), where we present the O-H distances which are most remarkably affected by the onset of the transition. According to the data in Table IV, we can expect the presence of the interatomic interactions between O and H with considerable strengths, since van der Waals distance for the O-H distance is given to be 2.7 Å.[19] The most of the O-H interatomic distances are reduced at low temperatures below T_c. Especially, the distances related to the oxygen atoms O_1 and O_4 are remarkably reduced, where the positions of these oxygen atoms are most influenced by the quenching of the rotational motion of the ClO_4^- tetrahedron with the Cl-O_3 rotational axis. It should be also noted that the O-H distances affected by the transition most belong to the BEDT-TTF molecules (A) on an inversion center. Therefore, this fact suggests that the quenching of the thermal motions of the ClO_4^- anions and the BEDT-TTF molecules induces the development of the intermolecular interaction network associated with the O-H atomic contacts between the BEDT-TTF molecules and the ClO_4^- anions. Figure 10 shows the change in the geometry concerning the ethylene groups and the ClO_4^- anions in the bc^* plane. As easily seen in Fig. 10, the development of the intermolecular interaction network below T_c makes short the intermolecular distances between the BEDT-TTF molecules and the ClO_4^- anions in the direction parallel to the c axis, resulting in the remarkable shrinkage of the c axis lattice constant, consistent with the present x-ray-diffraction measurements. Namely, the thermal contraction in the c-axis lattice parameter is five times as large as that of the b or a axis. Taking into account that the BEDT-TTF molecular planes are oriented approximately perpendicular to the conducting bc plane, the anisotropic thermal contraction induces rotations of the BEDT-TTF molecular planes with the rotational axis perpendicular to the bc plane. The rotation of the ClO_4^-

TABLE III. The interatomic distances (Å) in the ClO_4^- anion after Refs. 17 and 18. See Fig. 4 for the positions of the oxygen atoms.

	Cl-O_1	Cl-O_2	Cl-O_3	Cl-O_4	Average
Room temperature	1.412	1.388	1.407	1.408	1.404
120 K	1.448	1.455	1.433	1.435	1.443

TABLE IV. The interatomic distances (Å) between the hydrogen atoms of the ethylene groups in the BEDT-TTF molecules and the oxygen atoms of the ClO_4^- anion after Refs. 17 and 18. See Figs. 4 and 10 for the positions of the constituent atoms.

	Room temperature	120 K		Room temperature	120 K
O_1-H_3	2.63	2.30	O_4-H_2	2.96	2.57
O_1-H_5	2.91	2.95	O_4-H_3	2.50	2.41
O_1-H_6	2.77	2.82	O_4-H_9	2.97	2.62
O_3-H_1	2.48	2.38	O_4-H_{11}	2.90	2.46
O_3-H_6	2.59	2.71	O_4-H_8	2.82	2.90

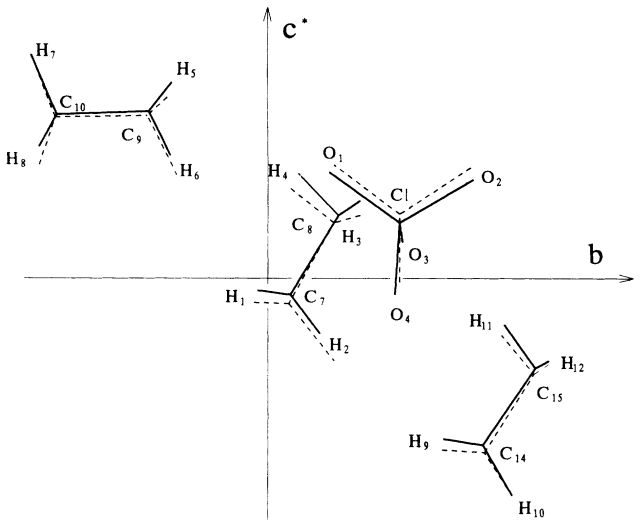

FIG. 10. The geometry of the ethylene groups of the BEDT-TTF molecules and the ClO_4^- ion in the *bc** plane at room temperature (dashed lines) and 120 K (solid lines) after Refs. 17 and 18. See Fig. 4 for the positions of the atoms.

ion is correlated to the rotation of the BEDT-TTF molecular plane in the *bc* plane through O-H intermolecular interactions, where the long axes of the BEDT-TTF molecules are approximately perpendicular to the *bc* plane. Although the estimation of the *g* tensors has some ambiguity at room temperature because of the asymmetric line shapes, the *g*-tensor analysis and the temperature dependence of the *g* values suggest that the metal-semiconductor transition makes the orientation of BEDT-TTF molecules changed in such a manner that the molecular plane rotates along the molecular long axis nearly perpendicular to the *bc* plane, consistent with the x-ray crystal structure analyses (Refs. 17 and 18) mentioned above. The correlated motions of the ethylene groups and the ClO_4^- ions deform the crystal structure, resulting in the steep decrease in the angle α at T_c and the large thermal contraction of the *c*-axis lattice constant. The rotations of the BEDT-TTF molecular planes modify the magnitudes of transfer integrals for the HOMO orbitals between the adjacent BEDT-TTF molecules, leading to the onset of the metal-semiconductor transition through a change in the electronic structure.

Now, we discuss again the transition in relation to the entropy change associated with the structural degrees of freedom. In the BEDT-TTF complex, ethylene groups have two kinds of configurations due to the nonplanarity of the BEDT-TTF molecule,[20] which are convertible through a bending motion of the ethylene group. According to the x-ray structural investigations[3,17,18] in $(BEDT\text{-}TTF)_3(ClO_4)_2$, the ethylene group is thermally vibrating at room temperature, and the lowering of the temperature makes thermal motion quenched below T_c. Therefore, if the thermal vibration of the ethylene group is completely quenched at T_c, the entropy change is given to be $R\ln 2 = 5.76$ J/K mol. $(BEDT\text{-}TTF)_3(ClO_4)_2$ has three BEDT-TTF molecules, each of which has two ethylene groups. Thus, the total entropy change for the BEDT-TTF molecules is expected to be $6R\ln 2$, if the transition makes the bending motions completely quenched for all the ethylene groups. Moreover, the rotational degree of freedom for the ClO_4^- anions is also expected to participate in the entropy change. As discussed in the above, the molecular motion of the ClO_4^- anion is considered to be expressed in terms of the hindered rotation with the three potential minima and the rotational axis of Cl-O_3. Therefore, if the rotation is completely quenched, a ClO_4^- anion gives the entropy change of $R\ln 3 = 9.13$ J/K mol. Taking into account the degrees of freedom both for the bending motion of the ethylene groups and the hindered rotation of the ClO_4^- anion, the total entropy change is expected to be $(6R\ln 2 + 2R\ln 3) = 52.82$ J/K mol if these molecular motions are completely quenched by the onset of the transition. Judging from the experimental fact that the observed value (3 J/K mol) of the total entropy change is more than 1 order of magnitude smaller than the expected value and involves the electronic entropy change, an incomplete quenching of the molecular motions is considered to be generated by the metal-semiconductor transition.

Here, we discuss the fact that the ESR line shape becomes anomalously asymmetric in the critical region of the transition as shown in Fig. 6(a). The asymmetric line shapes in the critical region behave differently from the metallic region well above T_c, namely, the asymmetric line shapes appear irrespective of the direction of the electric field of a microwave. There is no anomalous enhancement in dc and microwave conductivities (9 GHz) in the critical region around T_c, which will be expected if the asymmetric line shapes are caused by high conductivities. Therefore, the origin of the asymmetric line shapes is not ascribed to high conductivities, but to the enhancement of dielectric constants in the vicinity of T_c. The metal-semiconductor transition is correlated to the displacements of BEDT-TTF molecules which are linked to the development of the three-dimensional intermolecular interaction network between the donors and ClO_4^- anions as mentioned above. The anomalous enhancement in the dielectric constants suggests the dynamical behavior of the molecular motions in the vicinity of the transition.

Finally, we mention the anomaly in the specific heat observed around 120 K. In connection with the anomaly, we observe a small hump in the ESR linewidth around the same temperature region.[4] Thermoelectric power also gives an anomalous behavior in the same temperature region, that is, the appearance of a minimum in thermoelectric power.[21] The anisotropy ratio ρ_b/ρ_c in resistivity between the two crystallographic axes *b* and *c* in the conductive plane starts increasing below about 120 K.[21] This trend is consistent with the large thermal contraction in the *c*-axis lattice constant at low temperatures, since the *c*-axis thermal contraction makes electrical conduction in the *c*-axis direction enhanced through an in-

crease in the transfer integrals of the adjacent BEDT-TTF HOMO orbitals. Taking into account these experimental facts, it is speculated that a small structural change contributes to the anomaly since the thermal motions still survive in this temperature range according to the incomplete quenching of the thermal motions at T_c mentioned above.

SUMMARY

$(BEDT\text{-}TTF)_3(ClO_4)_2$ is a two-dimensional organic metal with conducting planes parallel to the *bc* plane, which has a metal-semiconductor transition at $T_c = 170.4$ K. We investigate the metal-semiconductor transition by means of specific heats, conductivities, ESR, and x-ray diffractions. The results of the specific heats suggest the second-order nature of the transition having a large entropy change. The x-ray diffractions prove anisotropic thermal contraction where the *c*-axis lattice constant has the largest thermal contraction. In addition to the H/D isotope effect on T_c, this result is related to the development of the intermolecular interaction network between ethylene groups of BEDT-TTF donors and ClO_4^- anions below T_c and consequently to the rotations of BEDT-TTF molecular planes with the rotational axis approximately parallel to the *a* axis. The displacements of BEDT-TTF molecules are ascertained by the abrupt change in the *g* tensors and their principal axes at T_c. We observe an anomalous enhancement in dielectric constants in the vicinity of T_c, which suggests the presence of dynamical behaviors in the molecular displacements in the critical region. Therefore, from the structural aspect, the metal-semiconductor transition consists of the three-dimensional structural phase transition correlated with the development of the intermolecular interaction network between ethylene groups of BEDT-TTF molecules and ClO_4^- anions.

ACKNOWLEDGMENTS

The authors would like to express their sincere thanks to Professor H. Kobayashi and Professor T. Mori for fruitful discussion and kind offers of their x-ray data. They also thank Dr. A. Miyazaki for his valuable suggestion. The ESR measurements were carried out using the facilities at the Institute for Molecular Science with kind assistance of Dr. S. Bando. This work was partly supported by the Grant-in-Aid for Scientific Research No. 03740611 from the Ministry of Education, Science and Culture, Japan.

[1] *The Physics and Chemistry of Organic Superconductors*, edited by G. Saito and S. Kagoshima (Springer-Verlag, Berlin, 1990).
[2] Y. Maniwa, T. Takahashi, and G. Saito, J. Phys. Soc. Jpn. **55**, 47 (1986).
[3] H. Kobayashi, R. Kato, T. Mori, A. Kobayashi, Y. Sasaki, G. Saito, T. Enoki, and H. Inokuchi, Chem. Lett. **1948**, 179 (1984).
[4] T. Enoki, K. Imaeda, M. Kobayashi, G. Saito, and H. Inokuchi, Phys. Rev. B **33**, 1553 (1986).
[5] S. S. P. Parkin, M. Miljak, and J. R. Cooper, Phys. Rev. B **34**, 1485 (1986).
[6] M. Kobayashi, T. Enoki, K. Imaeda, H. Inokuchi, and G. Saito, Phys. Rev. B **36**, 1457 (1987).
[7] H. Tajima, H. Kanbara, K. Yakushi, H. Kuroda, G. Saito, and T. Mori, Synth. Met. **25**, 323 (1988).
[8] T. Enoki, K. Tsujikawa, K. Suzuki, A. Uchida, and Y. Ohashi, Synth. Met. **56**, 2353 (1993).
[9] M. Tinkham, *Introduction to Superconductivity* (McGraw-Hill, New York, 1975).
[10] G. A. Samara, Ferroelectrics **20**, 87 (1978).
[11] M. Ichikawa, Chem. Phys. Lett. **79**, 583 (1981).
[12] K. Gesi, K. Ozawa, T. Osaka, and Y. Makita, J. Phys. Soc. Jpn. **52**, 2538 (1983).
[13] T. Sugano, G. Saito, and M. Kinoshita, Phys. Rev. B **34**, 117 (1986).
[14] H. E. Stanley, *Introduction to Phase Transitions and Critical Phenomena* (Clarendon, Oxford, 1971).
[15] R. A. Craven, M. B. Salamon, G. DePasquil, R. M. Herman, G. Stucky, and A. Schultz, Phys. Rev. Lett. **32**, 769 (1974).
[16] N. A. Fortune, K. Murata, M. Ishibashi, M. Tokumoto, N. Kinoshita, and H. Anzai, Solid State Commun. **77**, 265 (1991).
[17] H. Kobayashi (private communication).
[18] T. Mori (private communication).
[19] M. H. Whangbo and J. M. Williams, J. Am. Chem. Soc. **109**, 90 (1987).
[20] J. M. Williams, H. H. Wang, T. J. Emge, U. Geiser, M. A. Beno, P. C. W. Leung, K. D. Carlson, R. J. Thorn, A. J. Shultz, and M. H. Whangbo, Prog. Inorg. Chem. **35**, 51 (1987).
[21] K. Imaeda, T. Enoki, G. Saito, and H. Inokuchi, Bull. Chem. Soc. Jpn. **61**, 3332 (1988).